Dissolution of MWCNTs by Using Polyoxadiazoles, and Highly Effective Reinforcement of Their Composite Films

MARCIO R. LOOS,[1] VOLKER ABETZ,[1] KARL SCHULTE[2]

[1]Institute of Polymer Research, GKSS-Forschungszentrum Geesthacht GmbH, Max-Planck-Str. 1, 21502, Germany

[2]Institute of Polymer and Composites, Hamburg University of Technology, Denickestrasse 15, 21073, Germany

Received 26 May 2010; accepted 12 August 2010
DOI: 10.1002/pola.24315
Published online 5 October 2010 in Wiley Online Library (wileyonlinelibrary.com).

ABSTRACT: Nonmodified multiwalled carbon nanotubes (MWCNTs)/sulfonated polyoxadiazole (sPOD) nanocomposites are successfully prepared by a facile solution route. The pristine MWCNTs are dispersed in a sPOD solution, and the mixtures are fabricated into thin films by solution casting. The homogeneous dispersion of nanotubes in the composites is confirmed by transmission electron microscopy. The mechanical properties, thermal stability, and electrical conductivity are investigated. Tensile strength, elongation at break, and tensile energy to break are shown to increase by more than 28, 45, and 73%, respectively, by incorporating up to 1.0 wt % pristine MWCNTs. The experimental values for sPOD/MWCNTs composite stiffness are compared with Halpin-Tsai and modified Halpin-Tsai predictions. The storage modulus is found to increase up to 10% at low CNT loading. The composite films, which have an outstanding thermal stability, show an increase of up to 57 °C in the initial degradation temperature. The addition of 1.0 wt % MWCNTs increases the electrical conductivity of the sPOD matrix by two orders of magnitude. © 2010 Wiley Periodicals, Inc. J Polym Sci Part A: Polym Chem 48: 5172–5179, 2010

KEYWORDS: carbon nanotubes; composites; high performance polymers; mechanical properties; polyoxadiazoles

INTRODUCTION The outstanding properties of the carbon nanotubes make them a promising filler material to improve mechanical, thermal, and electrical properties of polymers. The key point is to transfer the potential properties of CNTs to the polymer composites. Due to the strong attractive long-ranged van der Waals interaction, nanotubes tend to aggregate and form bundles or ropes, usually with highly entangled network structure. Thus, despite of the high surface area of nanotubes that can act as desirable interface for stress transfer, it undesirably induces strong attractive forces between the CNTs themselves, leading to the excessive agglomeration behavior. In this context, two main issues are extremely important to the achievement of polymer composites with improved properties due to the addition of carbon nanotubes. These issues are the interfacial interaction between filler and polymer and the proper dispersion of the filler in the polymer matrix. A homogeneous dispersion of filler within the hosting matrix is a prerequisite of any composite. It is also vital to stabilize the dispersion to prevent re-aggregation of the filler.

There are four prominent methods for achieving dispersion of nanotubes: mechanical methods,[1] functionalizing the CNTs,[2] using surfactants,[3] and noncovalent modification by using small molecules and polymer dispersants.[4] There are, of course, advantages and disadvantages associated with each of these methods.[5] The use of noncovalent modification does not alter the properties of CNTs. However one potential drawback of noncovalent modification is that the dispersant must remain in the system to maintain the dispersion. This may not be desirable since the dispersant agent can alter the properties of the final composite, but if the dispersant can serve as a matrix, then noncovalent modification can be attractive.

Aromatic and aliphatic polymers such as polyimide,[5–8] polybenzimidazole,[4,9] polyaniline,[10,11] poly(arylene sulfone),[12] and sulfonated polyoxadiazoles (sPOD)[2] with conjugated groups have been reported to be excellent for dispersing CNTs in composites. This is due to the strong interfacial interactions (such as π-π interactions) between the conjugated groups of the polymer and the sidewall of the CNTs.

Aromatic poly(1,3,4-oxadiazole)s are a class of chemically resistant and thermally stable heterocyclic polymers.[13,14] They have been the focus of considerable interest with regard to the production of high-performance materials, particularly owing to their high thermal stability in oxidative atmosphere and specific properties determined by the structure of the 1,3,4-oxadiazole ring. Besides their excellent resistance to high temperature, polyoxadiazoles have many desirable characteristics, such as good hydrolytic stability, high glass transition temperatures, low dielectric constants, and tough mechanical properties.[13,15]

Present address: Department of Macromolecular Science and Engineering, Case Western Reserve University, Cleveland, Ohio 44106.
Correspondence to: M. R. Loos (E-mail: marcio.loos@case.edu).
Journal of Polymer Science: Part A: Polymer Chemistry, Vol. 48, 5172–5179 (2010) © 2010 Wiley Periodicals, Inc.

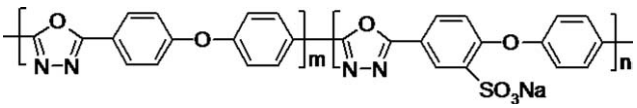

FIGURE 1 Chemical structure of poly(4,4′-diphenylether-1,3,4-oxadiazole)s (sPOD).

In this study, we describe the successful dispersion of multi-walled carbon nanotubes (MWCNTs) in a sulfonated poly(4,4′-diphenylether-1,3,4-oxadiazoles) (sPOD) matrix. The pristine MWCNTs are dispersed in a sPOD solution, and the mixtures are fabricated into thin film membranes by a solution casting method. The fine dispersion of the nanotubes throughout the polymer matrix as well as the improved interfacial interaction is found to improve the overall mechanical performance of the composites. Enhancements in thermal stability and electrical conductivity have been also achieved.

EXPERIMENTAL

Starting Materials

Pristine MWCNTs (CNT-MW) were purchased from Future Carbon and used as received. Poly(phosphoric acid) (115% H3PO4, Aldrich), hydrazine sulfate (>99%, Aldrich), dicarboxylic acid 4,4′-diphenylether, DPE (99%, Aldrich), dimethyl sulfoxide, DMSO (>99%, Aldrich), sodium hydroxide (99%, Vetec); all chemicals were used as received.

Preparation of sPOD/MWCNTs Composites

The synthesis of sPOD was performed following the process reported by Loos et al.[13,15] The molecular structure of the obtained sPOD, which has a molecular weight of 350,000 g mol^{-1} and a sulfonation level of 46%, is shown in Figure 1. sPOD/MWCNT nanocomposites containing different concentrations of filler (0.1, 0.5, and 1.0 wt %) were fabricated via a simple solution processing. In a typical experiment, sPOD (2.0 g) and the proper amount of CNTs were dissolved in DMSO and stirred overnight at 60 °C. The solutions were then sonicated at 60 °C for 1 h and casted on glass plates. After casting, the DMSO was evaporated at 90 °C for 24 h. For further residual solvent removal, the films were immersed in a water bath at 50 °C for 24 h and dried in a vacuum oven at 100 °C for 24 h. The final thickness of the films was about 60 μm.

Characterization

The morphology of the CNTs used in this work, as well as the nanocomposites, was analyzed with a transmission electron microscope (TEM). The TEM images were obtained using a Tecnai G2 F20 field emission transmission electron microscopy at an acceleration voltage of 200 kV. Dynamic mechanical thermal analysis (DMTA) was used for determination of the storage modulus (E'), loss modulus (E''), and loss tangent (tan δ) of the composite films. DMTA was performed using a TA instrument RSA 2 with a film tension mode at a frequency of 1 Hz and 0.1 N initial static force. The temperature was varied from 25 to 500 °C at a heating rate of 2 °C min^{-1} and at a constant strain of 0.05%. Tensile tests were performed according to the ASTM D882-00 using a Zwick-Roell equipment with a 500 N load cell. From the stress-strain curve, the tensile strength of the samples was estimated, and the elastic modulus calculated. At least 10 independent specimens from different films were investigated. The tensile energy to break (TEB), that is, the total energy absorbed per unit of volume of the specimen up to the point of rupture was also determined. Thermogravimetric analysis (TGA) experiments were carried out in a Netzsch 209 TGF1, equipped with a TASC 414/3 thermal analysis controller. The bulk sample, under argon and air atmosphere, was heated from 90 to 900 °C at 10 °C min^{-1}. The room temperature electrical conductivity of the composites was measured using a standard Van Der Pauw DC four probe method. The sample thickness was averaged over five measurements. Prior to the measurement, the corners of the samples with dimensions of 60 μm × 10 mm × 10 mm were coated with a thin silver paint. The current source was a Keithley 2061A apparatus.

RESULTS AND DISCUSSION

sPOD composites containing carbon nanotubes have been successfully prepared via solution processing. The proposed polyoxadiazole-MWCNTs interactions have been recently discussed elsewhere.[2] The noncovalent functionalization of nanotubes by sPOD is expected to happen by the interaction between aromatic groups from the diphenyl ether group with the CNTs, which is based on the ability of the extended π-system of the carbon nanotubes sidewall to bind guest molecules via π-π-stacking interactions.[2,5–8] Attempts to confirm the presence of an interaction between MWCNTs and sPOD were done by analyzing the FTIR spectra of the composites. Figure 2 shows a representative FTIR spectrum of the neat polyoxadiazole and sPOD/MWCNTs composites. No difference could be observed among the different MWCNTs compositions. The analysis of this figure indicates that no additional band and no shifted band can be detected for the composites. The two peaks at ~1600 cm and 1485 cm^{-1} arise from C=C stretching of the aromatic groups and are observed in all spectra. The asymmetric SO_2 stretch is observed at 1395 cm^{-1}. In covalent sulfonates, *R*-SO_2-OR, the asymmetric and symmetric SO_2 stretching

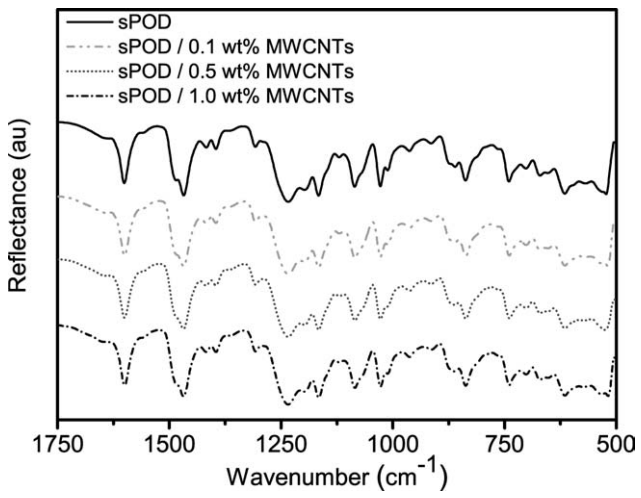

FIGURE 2 Representative FTIR spectra of the neat polyoxadiazole and of the sPOD/MWCNTs composites.

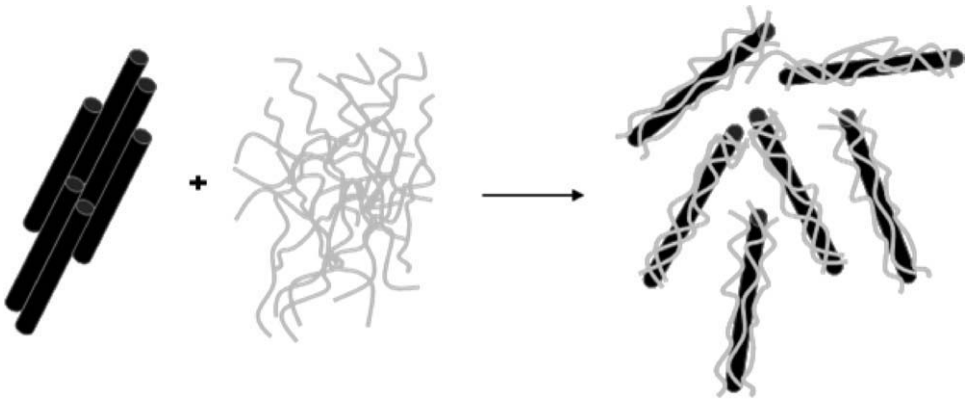

FIGURE 3 Schematic drawing of the interaction between sPOD and pristine MWCNTs.

vibration bands occur at 1415–1308 cm^{-1} and 1234–1145 cm^{-1}, respectively, whereas the asymmetric and symmetric SO stretching vibration bands occur at 1027–859 cm^{-1} and 837–670 cm^{-1}, respectively. The oxadiazole ring in the samples can be characterized through the assignments placed at 1468 and 1415 cm^{-1} related to the C=N stretching and by the assignment placed at 1085 cm^{-1} related to the —C—O—C— stretching.

The higher the interfacial interaction between the polymer and the dispersed nanofillers, the greater is the filler influence on the original characteristics of the polymer. In addition, the interaction polymer-nanotubes may prohibits the aggregation of the tubes resulting in a more stable suspension (Fig. 3).

The interactions of sPOD and MWCNTs enable the well dispersion of the nanotubes in the sPOD matrix. Figure 4 shows the appearance of sPOD/MWCNTs composites. The composites were placed on a paper printed with the words "GKSS Research Centre, Hamburg University of Technology—TUHH." The composites become darker in color with increasing nanotube content. Samples with 0.1 wt % MWCNTs still possess some optical clarity and visible by the naked eye, with uniform distribution of MWCNTs without any visible aggregate.

The homogeneous dispersion of nanotubes in the composites is confirmed by transmission electron microscopy. As shown in Figure 5, pristine MWCNTs are well dispersed as individual tubes in the sPOD matrix. It is worth noting that, as reported in the literature, pristine CNTs are usually found to be not well dispersed in different polymer matrices.[16,17]

Carbon nanotubes possess an extremely high tensile modulus (50–1000 GPa),[18–20] tensile strength (20–150 GPa),[21–23] and high aspect ratio (typically ~300–1000).[24] The addition of small amounts of CNTs to polymer matrices is expected to enhance the tensile properties significantly. The results of tensile tests obtained for the films of sPOD and sPOD/MWCNTs composites, in terms of Young's modulus (E), tensile strength (σ_M), and elongation at break (ε) with standard deviations and their percentage of increment are reported in Table 1. Figure 6 shows typical stress-strain curves obtained for the composites with various amounts of CNTs. The Young's modulus tends to increase for composites with 0.1 and 0.5 wt % MWCNTs. The tensile strength of sPOD is improved by 27% with the addition of just 0.1 wt % MWCNTs. Further increase in the CNT content does not produce further improvement in the tensile strength. More importantly, the ductility of sPOD is not compromised by the addition of pristine MWCNTs. Upon incorporation of only 0.1 wt % MWCNTs, the elongation at break of the composites increase by 35%, whereas the addition of 1.0 wt % CNTs further increase the aforementioned value by 45%. It is worth noting that the ductility and toughness of a polymer

FIGURE 4 Digital photographs of the neat polyoxadiazole and nanocomposites films reinforced with different amounts of MWCNTs.

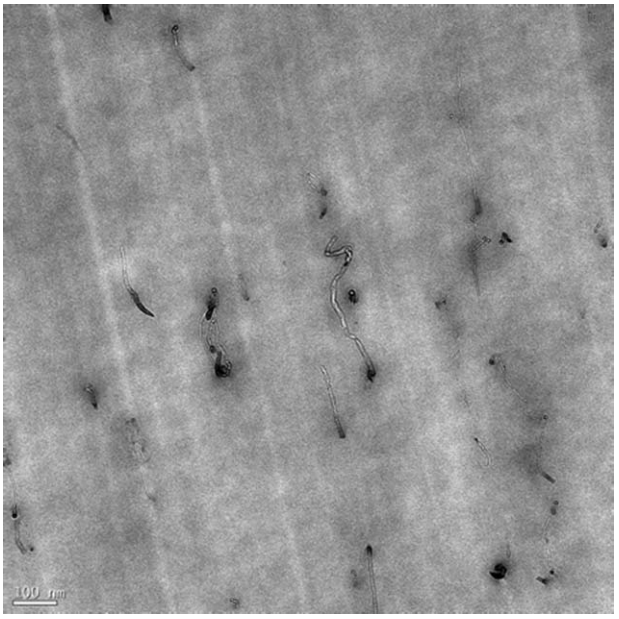

FIGURE 5 TEM images of sPOD composite reinforced with 0.5 wt % MWCNTs.

TABLE 1 Summary of Tensile Test Results for Neat sPOD and sPOD/MWCNTs Composites

MWCNTs (wt %)	E^a (Mpa)	$\sigma_M{}^b$ (Mpa)	σ_M Change (%)	ε^c (%)	ε Change (%)	TEB^d (MJ/m^3)	TEB Change (%)
0.0	2220 ± 152	173 ± 18	–	80 ± 14	–	103 ± 23	–
0.1	2320 ± 122	219 ± 8	+27	108 ± 8	+35	164 ± 17	+59
0.5	2370 ± 153	222 ± 11	+28	106 ± 9	+32	171 ± 21	+66
1.0	2240 ± 175	220 ± 9	+27	116 ± 8	+45	178 ± 17	+73

[a] Young's modulus.
[b] Tensile strength.
[c] Elongation at break.
[d] Tensile energy to break.

are usually reduced substantially upon the incorporation of non modified CNTs, as this have been reported in the literature for a large number of different polymer matrices.[25–27]

The effect of MWCNTs in the tensile performance of sPOD becomes even more clear by comparing the TEB of the neat polymer and composites (Table 1). As revealed by our results, the TEB increases with increasing nanotube loading in a linear fashion. An improvement of up to 73% at 1.0 wt % MWCNTs loading has been obtained. We attributed our success in enhancing the overall mechanical properties to the effective load transfer from the sPOD matrix to the MWCNTs as a result of the fine dispersion and interaction between the polymer and the CNTs.

We used two different equations to predict the Young's modulus of sPOD/MWCNTs composites. The Halpin-Tsai model has been used successfully to calculate the modulus of CNT reinforced polymer composites.[25,28] For randomly oriented CNTs in a polymer matrix, the modulus of the composite is given by the following equation[1,29,30]

$$\frac{E_C}{E_m} = \frac{3}{8}\left[\frac{1+2(l/d)\eta_L V_{NT}}{1-\eta_L V_{NT}}\right] + \frac{5}{8}\left[\frac{1+2\eta_T V_{NT}}{1-\eta_T V_{NT}}\right] \quad (1)$$

$$\eta_L = \frac{(E_{NT}/E_m)-1}{(E_{NT}/E_m)+2(l/d)}, \qquad \eta_T = \frac{(E_{NT}/E_m)-1}{(E_{NT}/E_m)+2} \quad (2)$$

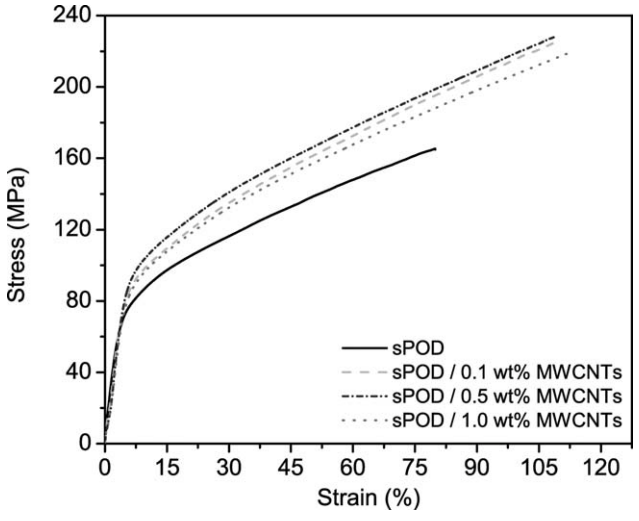

FIGURE 6 Representative stress-strain curves for the neat polyoxadiazole and nanocomposites.

where E_C, E_m, E_{NT} are the composite, matrix and CNT elastic modulus, respectively, V_{NT} is the CNT volume fraction and, l and d are the length and average outer diameter of the nanotube.

Thostenson and Chou[30] modified the Halpin-Tsai theory toward its applicability to nanotube reinforced composites. Considering that the outer wall of the nanotubes act as an effective solid fiber, with the same deformation behavior and diameter (d) and length (l) of the nanotube, the parameters η_L and η_T can be expressed as

$$\eta_L = \frac{(E_{NT}/E_m)-(d/4t)}{(E_{NT}/E_m)+(l/2t)}, \qquad \eta_T = \frac{(E_{NT}/E_m)-(d/4t)}{(E_{NT}/E_m)+(d/2t)} \quad (3)$$

where t is the thickness of graphite layer (0.34 nm).

The volume fraction of the nanotubes can be calculated according to

$$V_{NT} = \left[1+\left(\frac{\rho_{NT}}{\rho_m}\right)\left(\frac{1-m_{NT}}{m_{NT}}\right)\right]^{-1} \quad (4)$$

where m_{NT} is the weight fraction of the CNTs, and ρ_{NT} and ρ_m are the density of the CNTs and the polymer matrix, respectively.

The density of the CNTs can be calculated by assuming the graphitic layers of the tube shell to have the density of fully dense graphite ($\rho_g = 2.25$ g cm^{-3}), as suggested by Thostenson and Chou.[30]

$$\rho_{NT} = \rho_g \frac{(d^2 - d_i^2)}{d^2} \quad (5)$$

where, d_i is the inner diameter of the nanotube.

There is a large variation in modulus for CVD-MWCNTs reported in the literature with measured values ranging from 400 GPa[24] to just 50 GPa.[19] Nevertheless, the modulus strongly depends on the concentration of defects. As such, the experimental values for sPOD/MWCNTs composite stiffness are compared with Halpin-Tsai and modified Halpin-Tsai predictions using three different moduli of MWCNTs: 50, 100, and 400 GPa. During our simulations, the average length, outer, and internal diameter of the MWCNTs were taken to be $l = 10$ μm, $d = 15$ nm, and $d_i = 5$ nm, respectively. The value of ρ_{NT}/ρ_m was estimated to be 1.40. The comparison of experimental and theoretical values of stiffness is shown in Figure 7.

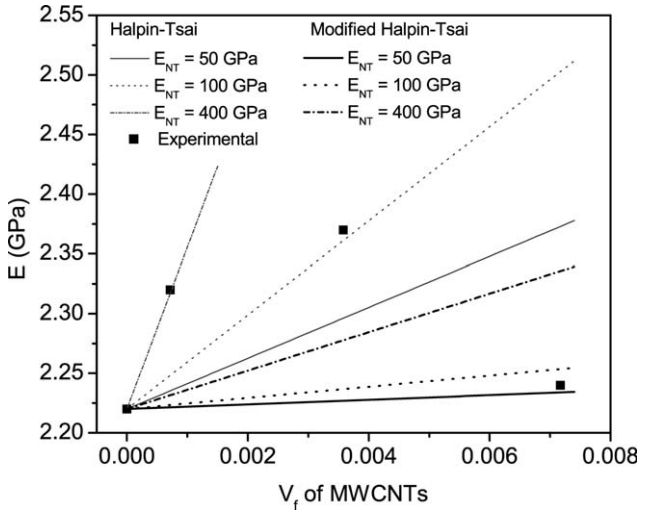

FIGURE 7 Theoretical Halpin-Tsai and modified Halpin-Tsai models and experimental data for the sPOD/MWCNTs composites at various nanotube loadings.

It can be seen that the modulus for composites with different MWCNT loadings lie between the calculated values. The experimental data for composites with 0.1 wt % (0.072 vol %) MWCNTs fits well with the Young's modulus calculated using the Halpin-Tsai equations if $E_{NT} = 400$ GPa. However, the increase in modulus with nanotube loading is not linear, and the Halpin-Tsai equations at $E_{NT} = 100$ GPa fits better the composite modulus at a loading of 0.5 wt % (0.036 vol %) MWCNTs. In the case of the sPOD composites containing 1.0 wt % (0.72 vol %) MWCNTs, there is a decrease in stiffness, and the experimental data fall between the values calculated using the modified Halpin-Tsai equations at $E_{NT} = 50$ GPa and $E_{NT} = 100$ GPa. It is worth noting that, according to the Halpin-Tsai equations, it is assumed that both CNTs and sPOD are very well bonded, equally strained and CNTs are homogeneously distributed within the sPOD.

The influence of pristine MWCNTs on the dynamical mechanical thermal behavior of the composites has been explored by DMTA. Figure 8 shows the temperature dependence of the storage modulus (E') and tan δ of sPOD and sPOD/MWCNTs composites, for different CNT loading. Similar dynamic mechanical spectra were recorded for the different samples. The storage modulus of pure sPOD decreases slowly and progressively with increasing temperature, showing a very strong decay in the temperature range between ~380 and 450 °C, which correlates with the glass transition of the polymer.

In most of the temperature range, the incorporation of MWCNTs induces a rise in the storage modulus of the matrix. In the case of composites containing 1.0 wt % MWCNTs, the aforementioned rise take place at temperatures higher than 140 °C [Fig. 8(a)]. Thus, at 100 °C, composites containing 0.1 and 0.5 wt % MWCNTs increased E' by approximately 7 and 10%, respectively. The observed enhancement in the mechanical response is attributed to the effective load transfer from the matrix to the filler likely resulting from an improvement in the MWCNTs dispersion. Analogous behavior has been reported in the literature for different polymer/CNT composites.[2,31] As can be seen in Table 2 and Figure 8(a), our results reveal a non linear growth of E' with nanotube amount, where the increase is more pronounced at low concentrations. At very low contents, the nanotubes are easier dispersed and therefore E' increases rapidly with MWCNT concentration. However, when the concentration becomes sufficiently large, the nanotubes can easily interact and may form small aggregates, which limit the interfacial area for stress transfer from the polymer matrix. Above the glass transition temperature, there are no obvious differences of the E' for the neat polymer and its composites.

Figure 8(b) shows representative curves for the tan δ as a function of temperature. In general, the glass transition temperature (T_g) of polymer/CNT composites depends on the interaction of reinforcement with the matrix, increasing with

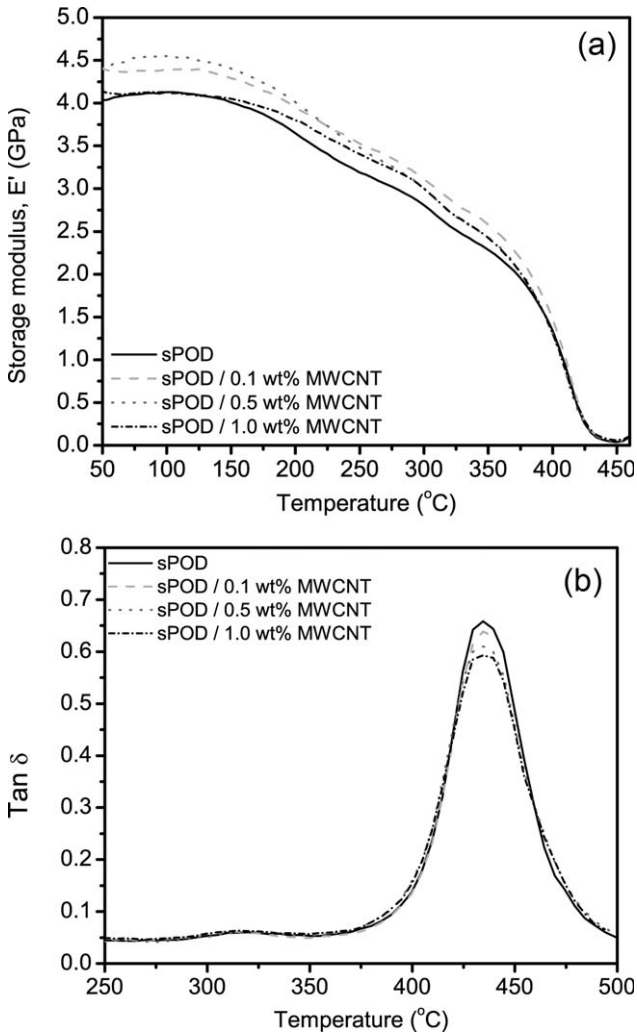

FIGURE 8 Dynamic mechanical analysis of composites: (a) storage modulus (E') and (b) tan δ of composites reinforced with pristine MWCNTs.

TABLE 2 Summary of DMTA Results, Thermal Stability, and Electrical Conductivity of sPOD Nanocomposites

	E' (Gpa)		T_g (°C)[a]		Char at 700 °C (%)		T_i (°C)[b]		
MWCNTs (wt %)	At 100 °C	At 300 °C	E''	tan δ	In Arg.	In Air	In Arg.	In Air	σ (S/m)
0.0	4.13	2.81	409	435	65	48	315	304	$6.4 \times 10^{-6} \pm 1 \times 10^{-6}$
0.1	4.39	3.11	409	435	65	47	338	321	$4.1 \times 10^{-6} \pm 7 \times 10^{-7}$
0.5	4.55	3.00	409	435	64	39	315	361	$4.4 \times 10^{-6} \pm 4 \times 10^{-7}$
1.0	4.13	3.00	409	435	64	49	327	326	$1.5 \times 10^{-4} \pm 3 \times 10^{-5}$

[a] Glass transition temperature measured by DMTA: loss modulus (E'') and tan δ.
[b] Initial degradation temperature obtained at 2% weight loss.

stronger interfacial interaction. In the case of sulfonated sPOD, the glass transition temperature is mainly determined by the ionic groups, present in the polymer chains and their interactions.[2,13]Furthermore, the use of different nanofillers has been found to have no significantly effect on the T_g of sPOD matrices.[2] As revealed by the results (Table 2), the glass transition temperature (measured either as the peak in the loss modulus curve or in the tan δ curve) of MWCNT reinforced samples results in no change of the T_g. Moreover, analysis of the magnitude of tan δ peaks indicates that the composites show progressive decreasing damping properties with increasing nanotube loadings. This is expected for nanotube reinforced composites because of the incorporation of completely elastic (tan $\delta \sim 0$) nanotubes in the polymer matrix. Similar behavior have been reported in the literature for CNT reinforced composites.[2,31] All experimental thermo mechanical data are tabulated in Table 2.

To study the thermal stability of the composites, TGA characterization has been carried out under dry air and argon atmospheres. The degradation curves of pure sPOD and composites containing 0.1, 0.5, and 1.0 wt % MWCNTs are displayed in Figure 9. It can be observed that the decomposition under inert environment takes place in a single stage, which involves decarboxylation and dehydration processes. The aromatic structures remain in the residue up to very high temperatures. At 700 °C, the residual amount in all composites is approximately 65% of the initial weight [Table 2, Fig. 9(a)]. Pure sPOD starts to degrade at 304 °C under argon and at 315 °C under air atmosphere. The incorporation of MWCNTs induces a thermal stabilization of the matrix under air; thus, the addition of 0.5 wt % CNTs increases the initial degradation temperature (Ti) up to 57 °C (Table 2). However, if we focus on the TGA under argon atmosphere, the increase in the aforementioned temperature is lower. The observed result reveals that a uniform and fine dispersion of the MWCNTs improves the interfacial adhesion between the CNTs and the matrix and restricts the thermal motion of the sPOD chains, thereby leading to composites thermally more stable. Furthermore, the CNTs may play a barrier effect which hinders the diffusion of the degradation products from the bulk of the polymer to the gas phase. Another explanation for the results could be the higher thermal conductivity of the composite that facilitates heat dissipation within the sample.

The electrical conductivity (σ) of the sPOD/MWCNTs nanocomposites as a function of MWCNT loading is shown in Table 2. As can be seen, the addition of 0.1 and 0.5 wt %

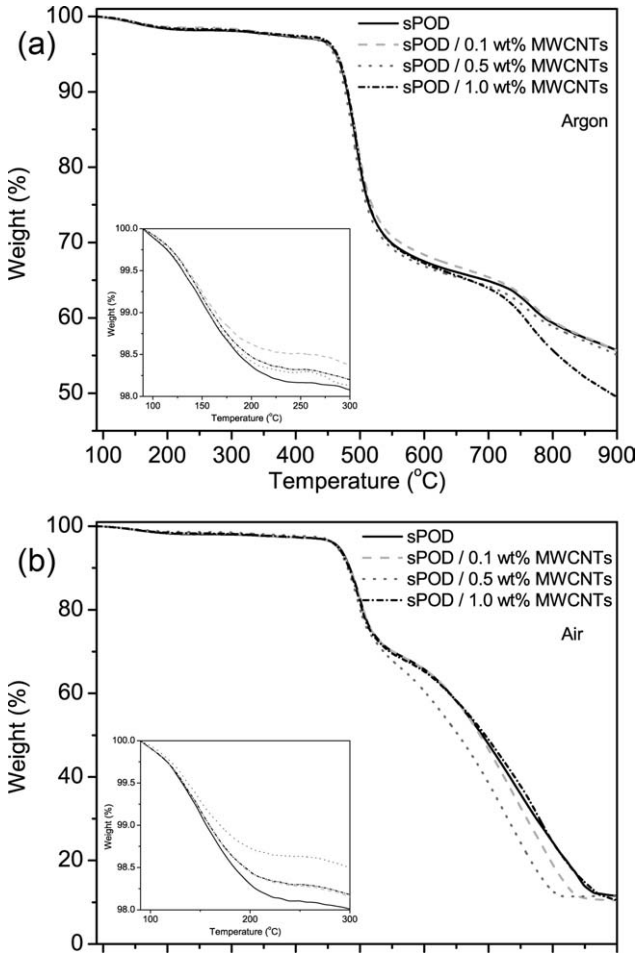

FIGURE 9 TGA curves of neat sPOD and sPOD/MWCNTs composites measured under (a) flowing argon and (b) air flow.

CNTs slightly decrease the electrical conductivity of the sPOD matrix. This apparent contradictory result may be a consequence of a complex interplay of the conductivity through the carbon nanotube network assisted by transport through carbon nanotube-bridging conjugated polymer chains.[32] The reason for this behavior is not fully understood. However, one suggestion is that the high affinity of the polymer for the CNTs surface allows the polymer to completely coat and insulate the CNT surface. Thus, the CNTs are coated with the semiconductor sPOD in such a way as to prevent the charge from transferring from one MWCNT to another. The observed conductivity could also be a result of the more uniform distribution of the MWCNTs, which in turn would decrease the likelihood of bundles touching to form a conductive network.[5] Similar results have been reported in the literature.[5,33] It is also worth noting that, as reported in the literature, conjugated polymer-based nanocomposites have presented lower levels of conductivity than insulating polymers after percolation.[34,35] Therefore, the behavior revealed by our results for the sPOD composites with 0.1 and 0.5 wt % is associated with charge transfer trough the semiconductor polymer.

Nevertheless, upon the addition of 1.0 wt % MWCNTs the sPOD matrix nanocomposites showed an increase of two orders of magnitude in electrical conductivity. This sharp increase observed in conductivity suggested the percolation threshold in the conductivity of the nanocomposites is above 0.5 wt %.

CONCLUSIONS

Pristine MWCNTs/sPOD nanocomposites were successfully prepared by a facile solution route. It was possible to achieve a homogeneous dispersion of nonmodified MWCNTs in the sPOD matrix, as confirmed by TEM. The investigation of tensile properties of the nanocomposites resulted in an increase of more than 28, 45, and 73% in tensile strength, elongation at break and TEB, respectively. The experimental values for sPOD/MWCNTs composite stiffness were fitted with Halpin-Tsai and modified Halpin-Tsai predictions. The storage modulus (at 100 °C) of composites containing 0.1 and 0.5 wt % MWCNTs was found to increase by approximately 7 and 10%, respectively. We attributed our success in enhancing the overall mechanical properties to the effective load transfer from the sPOD matrix to the MWCNTs. The obtained composite films, which have an outstanding thermal stability, have shown an increase of up to 57 °C in the initial degradation temperature. Furthermore, the addition of 1.0 wt % MWCNTs increased the electrical conductivity of the sPOD matrix by two orders of magnitude. The enhancement of the overall performance of the composites was found to be a result of the fine dispersion and interaction between the polymer and the CNTs.

The authors thank H. Böttcher for the DMTA and tensile tests, S. Neumann for the TGA analysis, M. Brinkmann for the SEC measurements, C. Abetz for the TEM images, and D. Gomes for the previous support.

REFERENCES AND NOTES

1 Gojny, F. H.; Wichmann, M. H. G.; Köpke, U.; Fiedler, B.; Schulte, K. Compos Sci Technol 2004, 64, 2363–2371.

2 Gomes, D.; Loos, M. R.; Wichmann, M. H. G.; de la Vega, A.; Schulte, K. Compos Sci Technol 2009, 69, 220–227.

3 Islam, M. F.; Rojas, E.; Bergey, D. M.; Johnson, A. T.; Yodh, A. G. Nano Lett 2003, 3, 269–273.

4 Li, N.; Zhang, F.; Wang, J.; Li, S.; Zhang, S. Polymer 2009, 50, 3600–3608.

5 Delozier, D. M.; Watson, K. A.; Smith J. G., Jr.; Clancy, T. C.; Connell, J. W. Macromolecules 2006, 39, 1731–1739.

6 Chen, H.; Liu, Z.; Cebe, P. Polymer 2009, 50, 872–880.

7 Licea-Jiménez, L.; Grishina, A. D.; Pereshivko, L. Y.; Krivenko, T. V.; Savelyev, V. V.; Rychwalski, R. W.; Vannikov, A. V. Carbon 2006, 44, 113–120.

8 Shigeta, M.; Komatsu, M.; Nakashima, N. Chem Phys Lett 2006, 418, 115–118.

9 Ishibashi, A.; Nakashima, N. Chem Eur J 2006, 12, 7595–7602.

10 Wu, T.-M.; Lin, Y.-W Carbon 2005, 43, 734–740.

11 Wang, G.; Ding, Y.; Wang, F.; Li, X.; Li, C. J Colloid Interface Sci 2008, 317, 199–205.

12 Joo, S. H.; Pak, C.; Kim, E. A.; Lee, Y. H.; Chang, H.; Seung, D.; Choi, Y. S.; Park, J.-B.; Kim, T. K. J Power Sources 2008, 180, 63–70.

13 Loos, M. R.; Gomes, D. High Perform Polym 2009, 21, 697–708.

14 Gomes, D.; Roeder, J.; Ponce, M. L.; Nunes, S. P. J Memb Sci 2007, 295, 121–129.

15 Gomes D. de F.; Loos, M. R. (GKSS Germany). U.S. Patent 12/369, 133, December 10, 2009.

16 Yang, B.-X.; Pramoda, K. P.; Xu, G. Q.; Goh, S. H. Adv Funct Mater 2062, 2007, 2062–2069.

17 Wang, M.; Pramoda, K. P.; Goh, S. H. Polymer 2005, 46, 11510–11516.

18 Popov, V. N. Mater Sci Eng 2004, 43, 61–102.

19 Salvetat, J.-P.; Kulik, A. J.; Bonard, J.-M.; Briggs, G. A. D.; Stöckli, T.; Méténier, K.; Bonnamy, S.; Béguin, F.; Burnham, N. A.; Forró, L. Adv Mater 1999, 11, 161–165.

20 Jeong, W.; Kessler, M. R. Chem Mater 2008, 20, 7060–7068.

21 Andrews, R.; Weisenberger, M. C.; Qian, D.; Meier, M. S.; Cassity, K. Nanomaterials: Inorganic and Bioinorganic Perspectives, vol. 1; Wiley: United Kingdom, 2009.

22 Stano, K.; Koziol, K.; Pick, M.; Motta, M.; Moisala, A.; Vilatela, J.; Frasier, S.; Windle, A. Int J Mater Form 2008, 1, 59–62.

23 Wagner, H. D. Chem Phys Lett 2002, 361, 57–61.

24 Xie, S.; Li, W.; Pan, Z.; Chang, B.; Sun, L. J Phys Chem Solids 2000, 61, 1153–1158.

25 Jeong, W.; Kessler, M. R. Carbon 2009, 47, 2406–2412.

26 Chen, G.-X.; Kim, H.-S.; Park, B. H.; Yoon, J.-S Polymer 2006, 47, 4760–4767.

27 Kim, K. H.; Jo, W. H. Compos Sci Technol 2008, 68, 2120–2124.

28 Kanagaraj, S.; Varanda, F. R.; Zhil'tsova, T. V.; Oliveira, M. S. A.; Simões, J. A. O. Compos Sci Technol 2007, 67, 3071–3077.

29 Peeterbroeck, S.; Breugelmans, L.; Alexandre, M.; Nagy, J. B.; Viville, P.; Lazzaroni, R. Compos Sci Technol 2007, 67, 1659–1665.

30 Thostenson, E. T.; Chou, T.-W. J Phys D Appl Phys 2003, 36, 573–582.

31 Chou, W.-J.; Wang, C.-C.; Chen, C.-Y. Compos Sci Technol 2008, 68, 2208–2213.

32 Musumeci, A. W.; Silva, G. G.; Liu, J.-W.; Martens, W. N.; Waclawik, E. R. Polymer 2007, 48, 1667–1678.

33 Haggenmueller, R.; Du, F.; Fischer, J. E.; Winey, K. I. Polymer 2006, 47, 2381–2388.

34 Kilbride, B. E.; Coleman, J. N.; Fraysse, J.; Fournet, P.; Cadek, M.; Drury, A.; Hutzler, S.; Roth, S.; Blau, W. J. J Appl Phys 2002, 92, 4024–4030.

35 Kymakis, E.; Amaratunga, G. A. J. J Appl Phys 2006, 99, 0843021–7.